How to cite: *Angew. Chem. Int. Ed.* **2025**, *64*, e202417308
doi.org/10.1002/anie.202417308

Electrochemical Interfaces

Adsorbate Resonance Induces Water-Metal Bonds in Electrochemical Interfaces

Marcus F. Nygaard[+], *Martin L. S. Nielsen*[+], *and Jan Rossmeisl**

Abstract: This study delves into the intricate interactions between surface-near species, OH and H_2O, on electrodes in electrochemical interfaces. These species are an inevitable part of many electrocatalytic energy conversion reactions such as the oxygen reduction reaction. In our modeling, we utilize high statistics on a dataset of complex solid solutions with high atomic variability to show the emergence of H_2O-metal covalent bonds under specific conditions. Based on density functional theory (DFT) calculations of adsorption energies on many thousands of different surface compositions, we provide a quantifiable physical understanding of this induced water covalency, which is rooted in simple quantum mechanics. Directional hydrogen bonding between surface-near H_2O and OH, enables surface bonding electrons to delocalize, mediated by near-symmetrical adsorbate resonance structures. The different adsorbate resonance structures differ by surface coordination explaining the induced H_2O-metal bonding.

Inside electrochemical cells, electricity is utilized to promote non-spontaneous electrochemical reactions, and inversely, their backwards reactions will release electricity. This is the foundation of electrochemistry ranging from chemical syntheses to sustainable energy solutions to mitigate climate change.[1] Ultimately, electrochemistry takes place in the spacing between the electrode and the electrolyte - the electrochemical interface - meaning that an accurate understanding hereof is of utmost importance.[2] Predominantly, electrolytes are aqueous solutions meaning that water molecules will be ever-present at the interface. As a result, water molecules are expected to impact reactions taking place in the cell - an effect we set forth to investigate in relation to the important and widely studied electrocatalytic oxygen reduction reaction (ORR).

The dominant catalytic theory for ORR activity is based on adsorption energy calculations between the bare catalyst surface and OH (ΔE_{*OH}) - an ORR intermediate. This is more commonly known as the descriptor-based approach.[3,4,5,6,7] However, the presence of water is challenging to encapsulate but has been explicitly accounted for both by means of static water descriptors,[8,9,10] ab initio molecular dynamics,[11,12,13] and grand canonical approaches.[14,15,16] These have revealed that water stabilizes *OH (* denoting adsorbed state) by a fixed amount, which was explained by the formation of hydrogen bonds between *OH and surface-near water, similar to those found in ice and liquid water.[17,18,19] As a consequence, explicit interfacial water was often excluded from *OH stability simulations but accounted for by an energy offset. However, we will show how this understanding becomes increasingly inaccurate for adsorption on heterogeneous surfaces as it overlooks a fundamental property of the adsorbates.[20,21,22]

We observe the emergence of undescribed interactions as water molecules from the interface approach a surface-bound *OH. The surface bonding electrons enter a superposition state where they bind both $*H_2O$ and *OH simultaneously. We coin this phenomenon, adsorbate resonance, and have provided a graphical representation of the relevant superposition in Scheme 1 to guide the conceptual understanding.

Adsorbate resonance gives rise to delocalized surface bonds that necessitate the use of multiple stability descriptors, and this happens because of an increased adsorbate stability due to said electron delocalization. We articulate this hypothesis using equation (1) to describe the adsorption of OH and surface-near water ($\Delta E_{*(OH-H_2O)}$):

$$\Delta E_{*(OH-H_2O)} = \Delta E_{mix} + \Delta E_{HBond} + \Delta E_{res} \quad (1)$$

The delocalized surface bond between *OH and $*H_2O$ would cause the adsorption energy to be described by a mix of multiple surface bonds (ΔE_{mix}). The formation of hydrogen bonds will inevitably stabilize the coadsorption of *OH and $*H_2O$ (ΔE_{HBond}), but it is expected that the delocalization due to adsorbate resonance would result in increased adsorption stability (ΔE_{res}). We devote the remainder of this communication to the relevant analyses and discussions of data, which enables us to test the hypothesis described by equation (1).

The basis for our study is a mixed adlayer of *OH and $*H_2O$, henceforth denoted $*(OH\text{-}H_2O)$. These species

[*] M. F. Nygaard,[+] M. L. S. Nielsen,[+] Prof. Ph. D. J. Rossmeisl
Center for High Entropy Alloy Catalysis (CHEAC), Department of Chemistry
University of Copenhagen
Universitetsparken 5, 2100 Copenhagen, Denmark
E-mail: jan.rossmeisl@chem.ku.dk

[+] These authors contributed equally to this work.

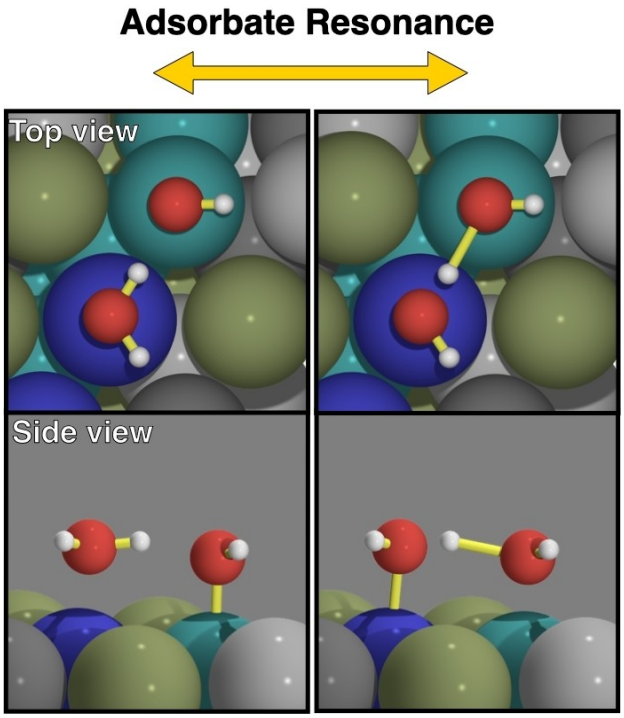

Scheme 1. Conceptual illustration of adsorbate resonance between two neighboring adsorbates, *OH and *H_2O, on a complex solid solution seen from the top and side by the upper and lower panel, respectively. The left and right sides differ only by the electronic configurations as indicated by the molecular and surface bonds (yellow cylinders) implying that they are resonance structures. We argue that the properties of adjacent *OH and *H_2O are best described as a superposition (linear combination) of said resonance structures.

preferably form a hexagonal pattern akin to a layer of ice (see Figure 1b).[23,24,25,26,27,28] Here, our method diverges from prior approaches by incorporating a vast number of multi-element alloys with random atomic arrangements also known as High-Entropy Alloys or Complex Solid Solutions (CSSs).[29,30] Unlike pure metals, the use of CSSs enables a statistical analysis where the binding sites of *OH and *H_2O can be changed independently giving rise to a large dataset, but more importantly it enables an energetic separation of *OH and *H_2O in the mixed adlayer.

By a comparison of different (co)adsorbate stabilities, the trends reveal that *(OH-H_2O) exhibit a striking similarity to the coadsorption of two OH adsorbates (see Supporting Information Figure S8), indicating that both *OH and *H_2O in the adlayer form surface bonds. Given this similarity, we present the underlying coadsorption data of *(OH-H_2O) in Figure 2 plotted against the *OH adsorption energy, $\Delta E_{*_{OH}}$, on the involved binding sites (See Supporting Information - computational details for more information).

Based on the data presented in Figure 2, we find that *H_2O and *OH couple into a common molecular entity inducing covalency between *H_2O and the surface causing a corresponding loss of the OH-surface bond. Conventionally, water has been considered to merely wet the surface with no surface bond formation whilst stabilizing *OH through hydrogen bonding (see Supporting Information Figure S2). Despite this comprehension, water covalency has previously been suggested,[14,27,32,33] but here we introduce a novel approach of leveraging high statistics (~5000 data points) combined with multiple linear regression to clearly demonstrate and for the first time quantify the existence of H_2O-surface bonds. We shall regard a "covalent bond" as the bond between an isolated OH and the surface ($\Delta E_{*_{OH}}$).

The linear coefficients arising from the regression highlight that the adsorption energy of *(OH-H_2O) correlates with a mix (ΔE_{mix}) of two fractional covalent bonds - approximately $\frac{2}{3}$ coming from *OH and $\frac{1}{3}$ from *H_2O. These fractional covalent bonds are evidence of induced H_2O-surface covalency. The sum of coefficients equals unity, meaning that the total bond order is one similar to that of isolated *OH. Furthermore, the fractional bonds highlight why mixed surface bonding is not directly observable on pure metal surfaces as $\Delta E_{mix} \approx \Delta E_{OH,pos1}$ when the involved sites are identical (i.e. $\Delta E_{OH,pos1} = \Delta E_{OH,pos2}$). The mixed surface bond gives *(OH-H_2O) bidentate adsorption characteristics. As a result, the adsorption energy spectrum of *(OH-H_2O) on CSSs is more homogeneous than its *OH counterpart (see Supporting Information Figure S11). With the discovery of a mixed adsorption descriptor, we tested and validated ΔE_{mix} among structures of larger unit cells, more adsorbates, and a higher compositional complexity (see Supporting Information Figure S3 and Figure S9).

From a structural analysis of the large adsorption dataset (see Supporting Information Table S2), we find trends supporting the induced covalency. Upon coadsorption, the internal O–H bonds in H_2O elongate by 3 % on average while the surface distance is reduced by 10 %. Conversely, the OH-surface distance increases by 7 % indicating a reduced bond. We also examined the hydrogen bonds presented in Figure 1. The *(H_2O^D-OH^A) hydrogen bond length is 0.3 Å shorter than in *(OH^D-H_2O^A). Finally, an internal bond angle expansion of 7.5 degrees for H_2O allows for better alignment with its hydrogen bond acceptors. These structural analyses point to an asymmetrical hydrogen bonding network and the importance of water as the donating species in the adlayer, similar to the conclusions drawn in other works.[26,31,32]

Given these insights, we examined whether the induced covalency could be exemplified by the pairwise adsorbate interactions, leading to an investigation of isolated dimers, trimers, and tetramers of adsorbates on the surface (see Supporting Information Table S1). Here, the H_2O covalency is observed to be present in an isolated *(H_2O^D-OH^A) adsorbate pairs where *H_2O^D forms $\frac{1}{6}$ covalent bond. For a *(H_2O^{DD}-$2OH^A$) adsorbate trimer, *H_2O^{DD} adsorbs with a strength of $\frac{1}{3}$ covalent bond as observed for the hexagonal network in Figure 2, which suggests an additive nature of the induced covalency. Curiously, as we exchange the roles of the interaction, *OH^D give rise to negligible covalency in *H_2O^A (see Supporting Information Table S1). We suggest that the absence and presence of water covalency are demonstrations of different adsorbate resonance structures. When it comes to the *(OH^D-H_2O^A) pair, its resonance structure is the charged *($O^{-,A}$-$H_3O^{+,D}$) (see Supporting

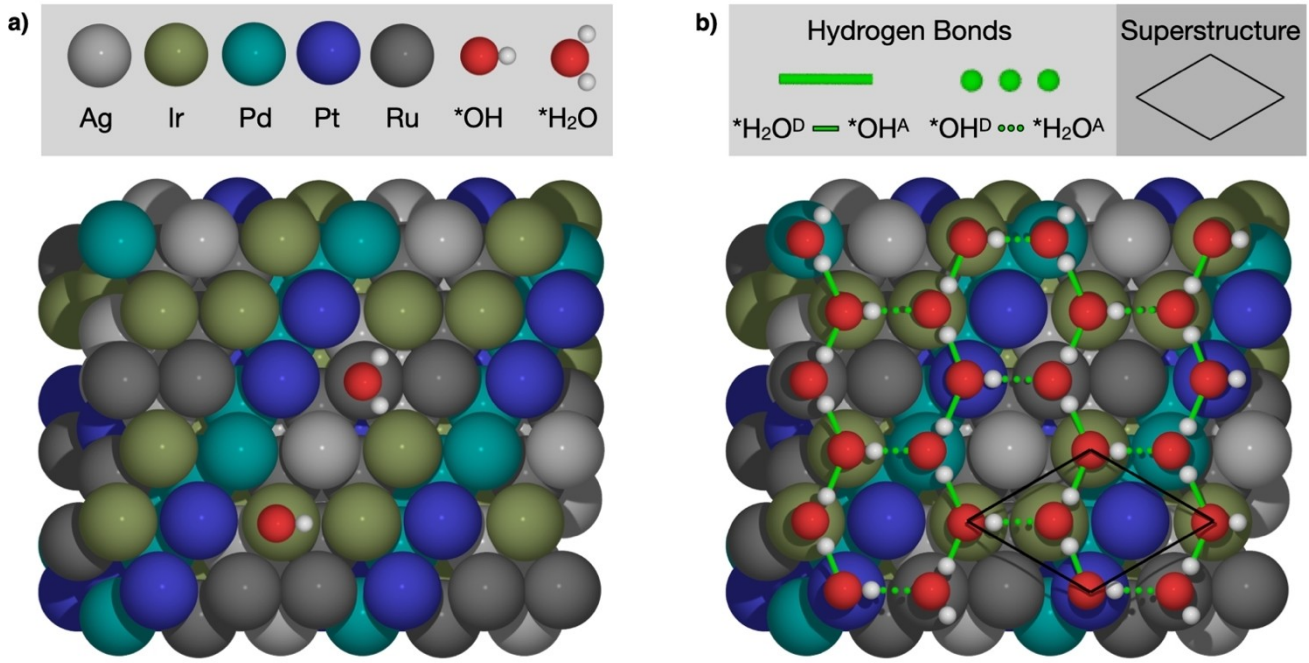

Figure 1. a) CSS with *OH and *H_2O. b) CSS with *(OH-H_2O) and the superstructure of the adlayer that imposes additional symmetry which unit cells must obey to reproduce hexagonal adlayers.

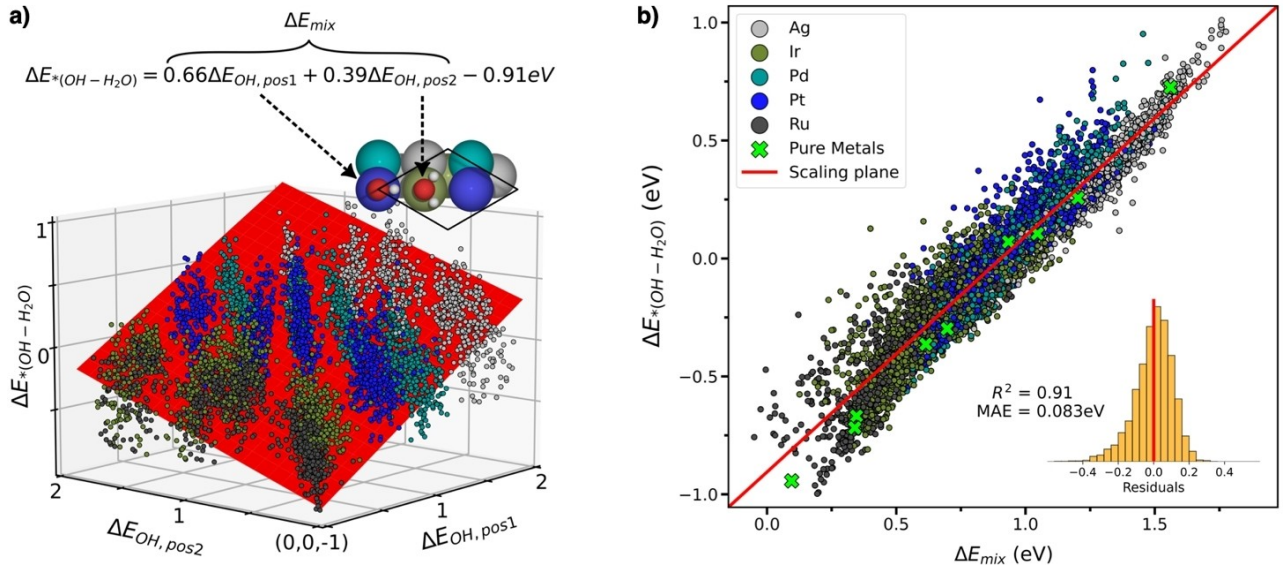

Figure 2. a) $\Delta E_{*(OH-H_2O)}$ versus the two relevant descriptors, $\Delta E_{OH,pos1}$ and $\Delta E_{OH,pos2}$ spanning the red scaling plane (see equation) colored by position 1 surface atoms. b) 2D representation of a) using the mixed descriptor i.e. ΔE_{mix} on the x-axis. The green crosses are pure metal data points (from low to high energy: Re, Ru, Ir, Rh, Pt, Pd, Ag, and Au). The inset shows a histogram of residuals when using the ΔE_{mix} descriptor to predict energies (see Supporting Information Figure S1 for a full version).

Information Figure S13). Besides an unfavorable charge formation, H_3O^+ should form no covalent surface bonds.

In contrast, *(H_2O^D-OH^A) is in resonance with what appears to be its own structural enantiomer, *(OH^A-H_2O^D), had it not been for an elongated internal bond in H_2O (see Scheme 1). Correspondingly, this process transfers the surface bond from one oxygen to the other. Being near-enantiomers, the resonance structures of *(H_2O^D-OH^A) must be close to degeneracy resulting in an electronic ground state wavefunction, which is a superposition of the two surface bonds seen in Scheme 1. Furthermore, this explains why the apparent bond order of the mixed descriptor, ΔE_{mix}, sums to unity as it is the same, single surface bond appearing at both binding sites. The delocaliza-

tion of electrons over the adjacent binding sites manifests itself in the electronic energies as seen in Figure 3.

Figure 3 provides an overview of the surface bond energy for six different adsorbate configurations with a bond order of unity. Comparing the *OH, *OH self-biting, and *(OH^D-H_2O^A) distributions to each other, a non-resonant hydrogen bond stabilizes adsorption without changing the characteristics of the distribution. Based on *(OH^D-H_2O^A) and *(H_2O-H_2O) adsorption data, we estimate the hydrogen bond energy, ΔE_{HBond}, on a surface without adsorbate resonance to be −0.16 eV on average (see Supporting Information Figure S12).

Interestingly, when reversing the donor/acceptor relationship of an adsorbate pair, we make two major energetic observations. First, the energy distribution of *(OH^D-H_2O^A) is clearly multimodal which contrasts *(H_2O^D-OH^A) adsorption where a smaller spacing and reduced relative intensity of the peaks make the distribution of adsorption energies appear increasingly homogeneous and unimodal. This is a natural consequence of the surface bond mixing for resonating adsorbates as described previously. Second, *(H_2O^D-OH^A) adsorption is significantly more stable than *(OH^D-H_2O^A) adsorption which highlights the importance of adsorbate resonance. Lastly, we examined the adsorption energy distributions of the zigzag and hexagonal adsorbate networks consisting of *OH and *H_2O. These networks constitute configurations with the most stable surface bonding due to the maximum number of adsorbate resonance structures. As such their distributions are exceptionally homogeneous and unimodal.

As evident in Figure 3 adsorbate resonance plays a major role in the energetics of the bonds between adsorbates and the surfaces. In equation 1, the *(OH-H_2O) adsorption energy was partitioned into three terms. Having accounted for ΔE_{mix} and ΔE_{HBond}, it is a simple task to distill the resonance energy in the adsorption data:

$$\Delta E_{res} = \Delta E*_{(OH-H_2O)} - (\Delta E_{mix} + \Delta E_{HBond}) \quad (2)$$

The resonance energy is defined as the residual of the observed *(OH-H_2O) adsorption energy once the mixed surface and hydrogen bonding terms have been subtracted. Equation (2) quantifies the stability gain of delocalized surface bonds.

In Figure 4, resonance energy distributions for different adsorbate configurations can be seen. Here it is evident that each pair of resonance structures stabilizes adsorption by ~-0.2 eV. For *(H_2O^D-OH^A), there is a single pair of resonance structures, whereas there are two pairs (one for each neighbor of H_2O) and thus double the resonance energy for the three other adlayers. This means that the resonance energy is ~-0.4 eV in *(H_2O^D-OH^A), the zigzag, and the hexagonal adlayer network. Based on this finding, it is suggested that even neighboring binding sites where their covalent bonding energies differ by 1 eV would find their *OH and *H_2O adsorbates resonating. This is the case for ruthenium and silver where the increased energy of $\frac{1}{6}$eV in ΔE_{mix} is fully compensated by the resonance energy (−0.2 eV). For heterogeneous CSSs of the five considered principal elements, adsorbate resonance is a universal phenomenon taking place in the electrochemical interface.

Based on our findings a natural question arises: Does adsorbate resonance break the scaling relations and thus the origin of the overpotential in ORR? In Figure S4 we reject this hypothesis by a demonstration of similar adsorbate

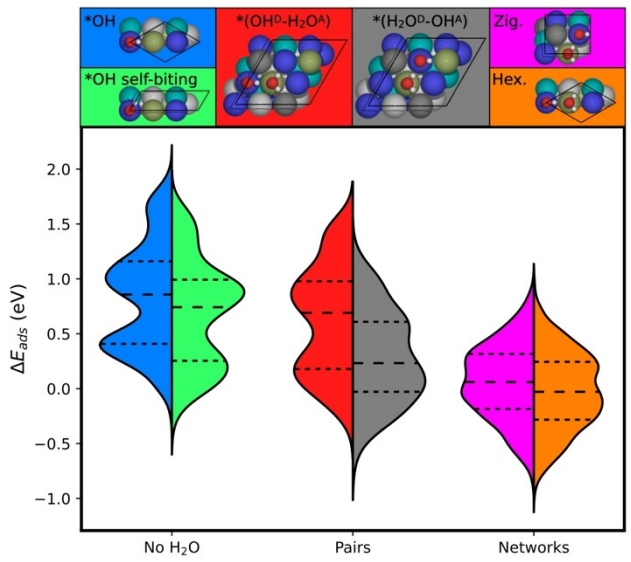

Figure 3. Estimated surface bond energy distributions for different adsorbate configurations with quartile indication by dashed lines (long dash represents the median). Within each violin, the left and right sides are normalized with respect to each other. All distributions involve calculations with a single (delocalized) surface bond which is also displayed in the graphical legend (top panel). Please note the subtle structure differences that arise by exchanging unit cells.

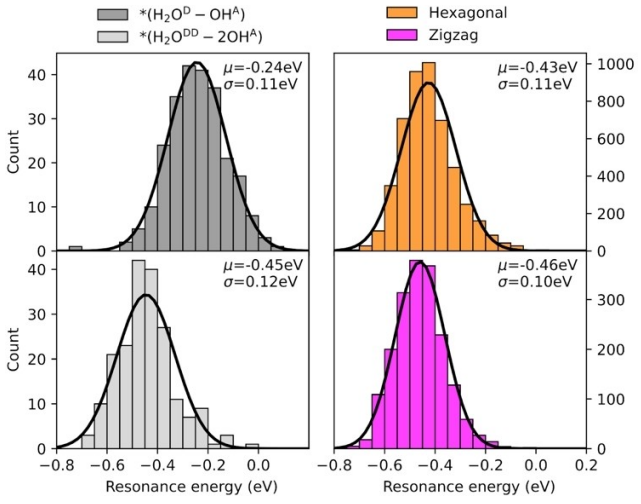

Figure 4. Resonance energy distributions for pairs, triplets and networks of resonating adsorbates. The black curves are the corresponding scaled normal distributions with the estimated mean (μ) and standard deviation (σ) seen in the top right corner for each distribution.

resonance in coadsorbed *OOH and *H_2O, which discloses that the scaling relation between *OH and *OOH when in the presence of water persists. However, adsorbate resonance could still impact surface design. Typically, three factors are considered to influence surface bonding of intermediates; the ensemble, the ligand, and strain effect caused by different binding sites, atomic neighborhood, and unit cell compression/expansion, respectively.[29,33] Based on our energetic analyses, we argue that adsorbate resonance is a predominant effect for *(OH-H_2O) adsorption on alloy surfaces. As shown in Figure S2b, omitting this effect leads to a skewed conception of the adsorption energetics. This work showcases the use of CSS as a tool to gauge catalytic theories as they present atomic and energetically diverse platforms where new theoretical discoveries loom. Similar analyses could be extended to transition states, wherein multiple effects impact its geometries. Lastly, we also find similar adsorbate resonance between coadsorbed water and methoxy (see Supporting Information Figure S5).

In this study we have uncovered a previously disguised effect in the *(OH-H_2O) interaction; adsorbate resonance induced covalency for water. This entails delocalized adsorbate-surface bonds across adjacent binding sites. Consequently, *(OH-H_2O) adsorption on heterogeneous surfaces adopts bidentate characteristics. Adsorbate resonance takes place in the *(H_2O^D-OH^A) configuration resulting in clearly preferred directionality in the interaction between *OH and *H_2O. We find that for each pair of resonance structures, the adsorption energy decreases by 0.2 eV. Since *H_2O can form two hydrogen bonds as a donor, it can partake in adsorbate resonance twice yielding a resonance energy of 0.4 eV in *(H_2O^{DD}-OH^A), the zigzag and hexagonal adlayer networks.

The adsorbate resonance sheds light on an important interaction in the near electrode region of the interface that was overlooked for pure metals, but now uncovered through high statistics and the large atomic variability in the surface of CSSs.

Supporting Information

The authors have cited additional references within the Supporting Information.[30,34,35,36,37,38,39,40,41,42,43,44,45]

Acknowledgements

All authors acknowledge financial the support from the Danish National Research Foundation Center for High-Entropy Alloy Catalysis (CHEAC) DNRF-149, the Deutsche Forschungsgemeinschaft (DFG, German Research Foundation) – SFB 1625 project number 506711657 subproject A01-Rossmeisl, and the European Union under ERC Synergy grant DEMI, GA no. 101118768.

Conflict of Interest

The authors declare no conflict of interest.

Data Availability Statement

The data that support the findings of this study are openly available in adsorbate resonance at https://sid.erda.dk/cgi-sid/ls.py?share_id=eXeLxj6RG4, reference number 214482816.

Keywords: Complex solid solutions · Computational Chemistry · Electrocatalysis · Electrochemical interface · Surface Chemistry

[1] I. Staffell, D. Scamman, A. V. Abad, P. Balcombe, P. E. Dodds, P. Ekins, N. Shah, K. R. Ward, *Energy Environ. Sci.* **2019**, *12*, 463–491.
[2] M. H. Hasan, I. T. McCrum, *Curr. Opin. Electrochem.* **2022**, *33*, 100937.
[3] P. Sabatier, *La Catalyse en chimie organique*, **1913**.
[4] J. N. Bronsted, *Chem. Rev.* **1928**, *5*, 231–338.
[5] M. G. Evans, M. Polanyi, *Trans. Faraday Soc.* **1936**, *32*, 1333.
[6] J. K. Nørskov, J. Rossmeisl, A. Logadottir, L. Lindqvist, J. R. Kitchin, T. Bligaard, H. Jónsson, *J. Phys. Chem. B.* **2004**, *108*, 17886–17892.
[7] F. Abild-Pedersen, J. Greeley, F. Studt, J. Rossmeisl, T. R. Munter, P. G. Moses, E. Skúlason, T. Bligaard, J. K. Nørskov, *Phys. Rev. Lett.* **2007**, *99*, 016105.
[8] A. Roudgar, A. Groß, *Chem. Phys. Lett.* **2005**, *409*, 157–162.
[9] S. Schnur, A. Groß, *New J. Phys.* **2009**, *11*, 125003.
[10] K. Tonigold, A. Groß, *J. Comput. Chem.* **2012**, *33*, 695–701.
[11] H. H. Kristoffersen, T. Vegge, H. A. Hansen, *Chem. Sci.* **2018**, *9*, 6912–6921.
[12] G. Di Liberto, L. Giordano, *Electrochem. Sci. Adv.* **2024**, *4*, e2100204.
[13] J. Le, M. Iannuzzi, A. Cuesta, J. Cheng, *Phys. Rev. Lett.* **2017**, *119*, 016801.
[14] M. H. Hansen, A. Nilsson, J. Rossmeisl, *Phys. Chem. Chem. Phys.* **2017**, *19*, 23505–23514.
[15] N. G. Hörmann, O. Andreussi, N. Marzari, *J. Chem. Phys.* **2019**, *150*, 041730.
[16] J. Huang, Y. Zhang, M. Li, A. Groß, S. Sakong, *J. Phys. Chem. Lett.* **2023**, *14*, 2354–2363.
[17] K. H. Kim, K. Amann-Winkel, N. Giovambattista, A. Späh, F. Perakis, H. Pathak, M. L. Parada, C. Yang, D. Mariedahl, T. Eklund, T. J. Lane, S. You, S. Jeong, M. Weston, J. H. Lee, I. Eom, M. Kim, J. Park, S. H. Chun, P. H. Poole, A. Nilsson, *Science* **2020**, *370*, 978–982.
[18] J. Yang, R. Dettori, J. P. F. Nunes, N. H. List, E. Biasin, M. Centurion, Z. Chen, A. A. Cordones, D. P. Deponte, T. F. Heinz, M. E. Kozina, K. Ledbetter, M.-F. Lin, A. M. Lindenberg, M. Mo, A. Nilsson, X. Shen, T. J. A. Wolf, D. Donadio, K. J. Gaffney, T. J. Martinez, X. Wang, *Nature* **2021**, *596*, 531–535.
[19] A. Rosu-Finsen, M. B. Davies, A. Amon, H. Wu, A. Sella, A. Michaelides, C. G. Salzmann, *Science* **2023**, *379*, 474–478.
[20] B. Cantor, I. T. H. Chang, P. Knight, A. J. B. Vincent, *Mater. Sci. Eng. A* **2004**, *375–377*, 213–218.
[21] J.-W. Yeh, S.-K. Chen, S.-J. Lin, J.-Y. Gan, T.-S. Chin, T.-T. Shun, C.-H. Tsau, S.-Y. Chang, *Adv. Eng. Mater.* **2004**, *6*, 299–303.

[22] T. A. A. Batchelor, J. K. Pedersen, S. H. Winther, I. E. Castelli, K. W. Jacobsen, J. Rossmeisl, *Joule* **2019**, *3*, 834–845.
[23] A. Michaelides, P. A. Hu, *J. Chem. Phys.* **2001**, *114*, 513–519.
[24] G. S. Karlberg, G. Wahnström, *J. Chem. Phys.* **2005**, *122*, 194705.
[25] A. Michaelides, *Appl. Phys. A* **2006**, *85*, 415–425.
[26] T. Schiros, H. Ogasawara, L.-Å. Näslund, K. J. Andersson, J. Ren, Sh. Meng, G. S. Karlberg, M. Odelius, A. Nilsson, L. G. M. Pettersson, *J. Phys. Chem. C* **2010**, *114*, 10240–10248.
[27] C. Clay, S. Haq, A. Hodgson, *Phys. Rev. Lett.* **2004**, *92*, 046102.
[28] S. Haq, J. Harnett, A. Hodgson, *Surf. Sci.* **2002**, *505*, 171–182.
[29] C. M. Clausen, T. A. A. Batchelor, J. K. Pedersen, J. Rossmeisl, *Adv. Sci.* **2021**, *8*, 2003357.
[30] C. M. Clausen, M. L. S. Nielsen, J. K. Pedersen, J. Rossmeisl, *High Entropy Alloys Mater.* **2023**, *1*, 120–133.
[31] M. Forster, R. Raval, J. Carrasco, A. Michaelides, A. Hodgson, *Chem. Sci.* **2012**, *3*, 93–102.
[32] J. Li, C. Q. Sun, *Mater. Today Adv.* **2021**, *12*, 100172.
[33] M. Escudero-Escribano, P. Malacrida, M. H. Hansen, U. G. Vej-Hansen, A. Velázquez-Palenzuela, V. Tripkovic, J. Schiøtz, J. Rossmeisl, I. E. L. Stephens, I. Chorkendorff, *Science* **2016**, *352*, 73–76.
[34] P. Hohenberg, W. Kohn, *Phys. Rev.* **1964**, *136*, B864–B871.
[35] W. Kohn, L. J. Sham, *Phys. Rev.* **1965**, *140*, A1133–A1138.
[36] B. Hammer, L. B. Hansen, J. K. Nørskov, *Phys. Rev. B* **1999**, *59*, 7413–7421.
[37] J. Enkovaara, C. Rostgaard, J. J. Mortensen, J. Chen, M. Dułak, L. Ferrighi, J. Gavnholt, C. Glinsvad, V. Haikola, H. A. Hansen, H. H. Kristoffersen, M. Kuisma, A. H. Larsen, L. Lehtovaara, M. Ljungberg, O. Lopez-Acevedo, P. G. Moses, J. Ojanen, T. Olsen, V. Petzold, N. A. Romero, J. Stausholm-Møller, M. Strange, G. A. Tritsaris, M. Vanin, M. Walter, B. Hammer, H. Häkkinen, G. K. H. Madsen, R. M. Nieminen, J. K. Nørskov, M. Puska, T. T. Rantala, J. Schiøtz, K. S. Thygesen, K. W. Jacobsen, *J. Phys. Condens. Matter* **2010**, *22*, 253202.
[38] J. Wellendorff, K. T. Lundgaard, A. Mogelhoj, V. Petzold, D. D. Landis, J. K. Norskov, T. Bligard, K. W. Jacobsen, *Phys Rev B* **2012**, *85*, 235149.
[39] A. H. Larsen, J. J. Mortensen, J. Blomqvist, I. E. Castelli, R. Christensen, M. Dułak, J. Friis, M. N. Groves, B. Hammer, C. Hargus, E. D. Hermes, P. C. Jennings, P. B. Jensen, J. Kermode, J. R. Kitchin, E. L. Kolsbjerg, J. Kubal, K. Kaasbjerg, S. Lysgaard, J. B. Maronsson, T. Maxson, T. Olsen, L. Pastewka, A. Peterson, C. Rostgaard, J. Schiøtz, O. Schütt, M. Strange, K. S. Thygesen, T. Vegge, L. Vilhelmsen, M. Walter, Z. Zeng, K. W. Jacobsen, *J. Phys. Condens. Matter* **2017**, *29*, 273002.
[40] C. M. Clausen, J. K. Pedersen, T. A. A. Batchelor, J. Rossmeisl, *Nano Res.* **2022**, *15*, 4775–4779.
[41] T. A. A. Batchelor, T. Löffler, B. Xiao, O. A. Krysiak, V. Strotkötter, J. K. Pedersen, C. M. Clausen, A. Savan, Y. Li, W. Schuhmann, J. Rossmeisl, A. Ludwig, *Angew. Chem. Int. Ed.* **2021**, *60*, 6932–6937.
[42] T. A. A. Batchelor, J. K. Pedersen, S. H. Winther, I. E. Castelli, K. W. Jacobsen, J. Rossmeisl, *Joule* **2019**, *3*, 834–845.
[43] H. J. Monkhorst, J. D. Pack, *Phys. Rev. B* **1976**, *13*, 5188–5192.
[44] J. D. Pack, H. J. Monkhorst, *Phys. Rev. B* **1977**, *16*, 1748–1749.
[45] J. K. Nørskov, J. Rossmeisl, A. Logadottir, L. Lindqvist, J. R. Kitchin, T. Bligaard, H. Jónsson, *J. Phys. Chem. B* **2004**, *108*, 17886–17892.

Manuscript received: September 9, 2024
Accepted manuscript online: October 17, 2024
Version of record online: November 11, 2024